Physica **44** (1969) 161–176 © *North-Holland Publishing Co., Amsterdam*

COLLISIONS OF Ar^+ IONS WITH Cu ATOMS IN THE VAPOUR PHASE

W. F. VAN DER WEG, D. J. BIERMAN and D. ONDERDELINDEN
FOM-Instituut voor Atoom- en Molecuulfysica, Amsterdam, Nederland

Received 11 February 1969

Synopsis

Measurements on the charge states of Ar and Cu ions resulting from collisions of 30–90 keV Ar^+ ions with Cu vapour are presented as a function of scattering angle. The results are compared with calculations according to a statistical model for the distribution of inelastic energy loss among the electrons of the collision partners. Expressions for the degree of ionization using a staggered ionization potential model have been derived. The treatment is largely based upon Russek's model and may be compared with Everhart's description of the $Ar^+ \rightarrow Ar$ collision. The amount of inelastic energy, according to the model, necessary for the multiple ionization, is compared with earlier measurements.

This paper, together with the inelastic energy measurements constitutes a phenomenological description of the $Ar^+ \rightarrow Cu$ collisions.

1. *Introduction.* Much research has been carried out on the analysis of heavy particle collisions in the keV region. These studies were primarily concerned with binary encounters between an ion and an atom in a gas[1,2]).

On the other hand, also binary collisions of ions with atoms situated on a metal surface were studied[3–5]). An important conclusion could be drawn from the comparison of collisions on a metal and in a gas. The kinetic energy of scattered particles and also the inelastic energy loss, dissipated over both partners, during a collision between a fast ion and a target atom do not depend on the physical state of the target. However, the charge state of scattered particles depends strongly on the nature of the target. It was reported some years ago[6]) that the mean charge of Ar ions scattered from gaseous Cu atoms is in the order of 5 for scattering angles larger than 30° and primary energy of 90 keV, whereas this mean charge is 2.5 for the case of scattering from a metal.

In order to explain these differences an analysis of the Ar^+ on Cu (gas) collision will be given in this paper and the Ar^+ on Cu (metal) collision will be discussed in the following paper.

The model used in this paper to describe the collision of an Ar^+ ion with

a free Cu atom is the model introduced by Everhart and Kessel[7]), which is an extension of Russek's description of atomic collisions. Coincidence techniques could not be used, because in case of a metal target one of both collision partners always disappears into the target. Therefore, no detailed information about the collision process can be extracted from the measurements, but a phenomenological description can be given.

We studied the reaction

$$Ar^{+} + Cu\ (gas) \rightarrow Ar^{m+} + Cu^{n+} + (m + n - 1)\,e$$

for scattering angles φ between 0° and 105° and primary energies between 30 and 90 keV.

2. *Apparatus.* The ion accelerator, scattering chamber and analyzing system is described already in connection with measurements of the inelastic energy loss of Ar^{+} ions in collision with gaseous and solid Cu targets[5]).

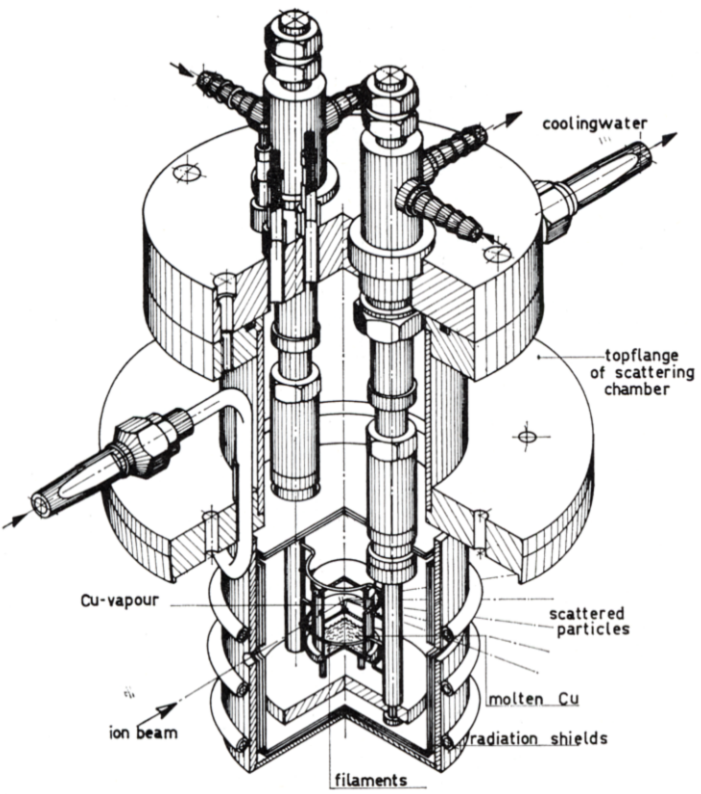

Fig. 1. View of oven and current supplies.
The Mo crucible is heated by electron bombardment from tungsten filaments, which are kept at −1 kV with respect to the crucible. Radiation shields and cooling system are indicated.

To produce Cu vapour an oven is inserted in the scattering chamber (fig. 1). It consists of a molybdenum crucible which is heated by electron bombardment. The primary ion beam is directed into the crucible, the scattered particles leave the crucible through a slit, after which they enter a region between grounded plates (not indicated in the figure) on their way to the diaphragm of the analyzer. It is necessary to construct this field-free region to make sure that the filament potential (1 kV) does not disturb the ion trajectories.

A chromel alumel thermocouple regulates the filament current so that the oven temperature can be stabilized within 2°C in the temperature region 1000°–1250°C. The partial pressure of the Cu vapour in our experiments was in the order of 10^{-4} torr. To be sure that the vapour pressure was low enough to work under single collision conditions, scattered ion intensities as a function of pressure were measured. A linear dependence of intensities on pressure was found.

The scattered ions pass an electrostatic energy analyzer and are detected by a Bendix particle multiplier. Neutral particles reach a detector by a hole in the analyzer plate.

We assume the multiplication factor of the multiplier to be independent of the charge of incoming ions. For slow ions (kinetic energy < 2 keV) this is certainly not the case, because acceleration of charged particles near the anode of the multiplier becomes important.

There is evidence for this effect in the measurement of intensities of slow recoil particles.

3. *Measurements.* We define the fraction P_n of scattered particles with charge n as the yield of n-times charged particles divided by the yield of these particles summed over all charge states.

It is measured as a function of scattering angle for 4 different primary energies. P_n values for projectile particles are given in fig. 2a.

It is observed that for increasing violence of the collision, higher charge states become predominant. This occurs for fixed primary energy with increasing scattering angle and for fixed scattering angle with increasing primary energy.

The neutral species are not indicated in some cases, they could not be measured accurately as a result of a large background (presumably photons). This introduces an error of some percents in the region of scattering angles 2°–10°.

Similar measurements on recoil Cu ions are presented in fig. 2b for three primary energies. Now the most violent collisions resulting in high-charge states occur for decreasing scattering angles with fixed energy and also for increasing primary energy with fixed scattering angle. The results for Cu are much more fragmentary than for Ar for two reasons. Firstly, in the

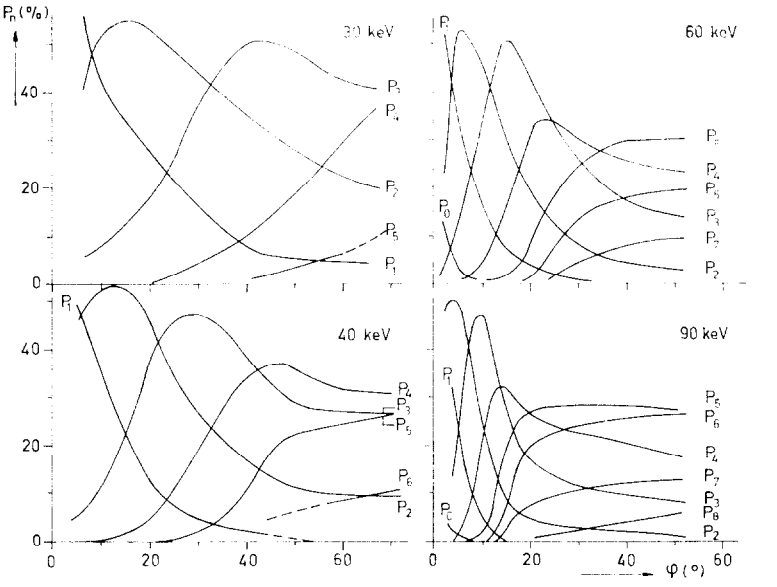

a

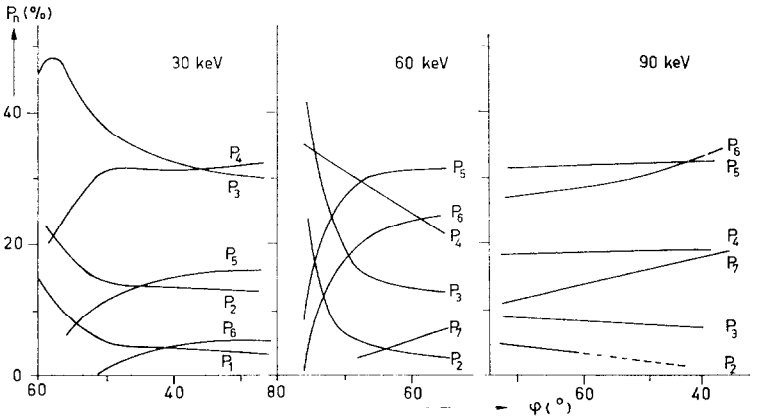

b

Fig. 2. Measured P_n functions *vs* laboratory scattering angle.
a) P_n functions for scattered Ar for 4 primary energies.
b) P_n functions for scattered Cu for 3 primary energies.
The curves are drawn through points, measured with intervals of 4°.

region of small scattering angles ($\varphi < 50°$) the differential cross section for scattering of a recoil into φ is small (compared to the cross section for scattering of a projectile particle into angle φ), so an intensity problem arises.

On the other hand, the region of scattering angles near 90° corresponds

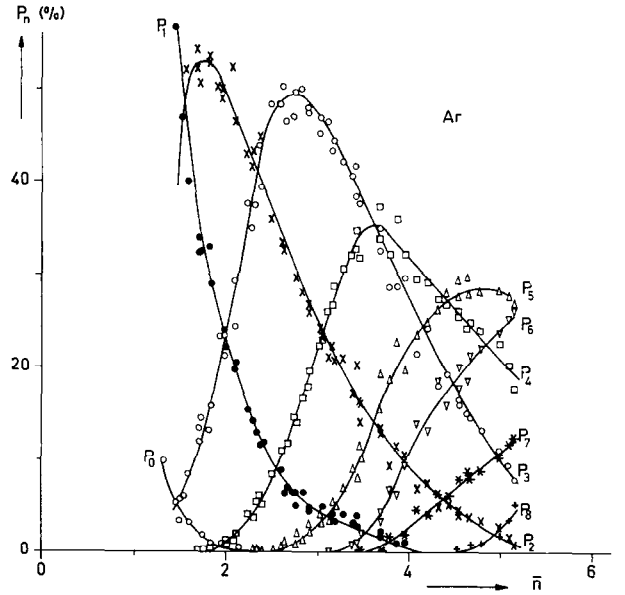

a

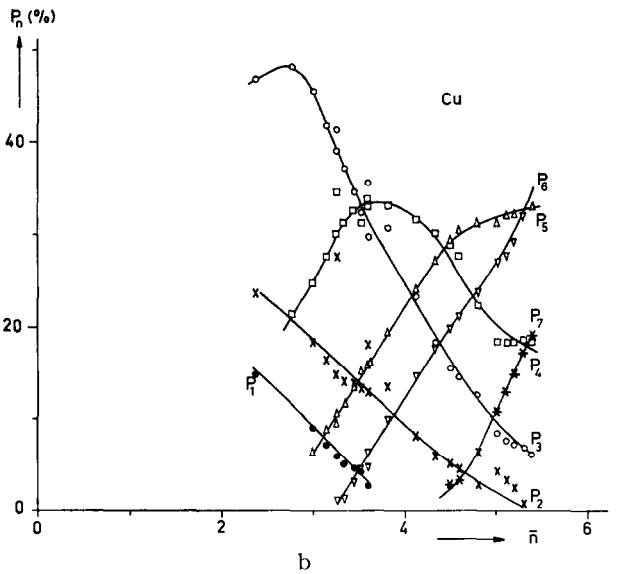

b

Fig. 3.

a) P_n functions plotted *vs* mean charge $\bar{n}$ for Ar.
Experimental points taken at 4 primary energies are combined in each curve.

b) P_n functions plotted *vs* $\bar{n}$ for Cu. Experimental points for 3 primary energies are combined in the curves.

Figure 3 is derived from fig. 2 by determining $\bar{n}$ for each φ.

with very low energies (recoil particle energy is proportional to $\cos^2 \varphi$) of scattered recoil particles for which the efficiency of the particle multiplier decreases below unity. Reacceleration of ions near the multiplier entrance grid plays a role here. As a result the measurements of relative ion intensities are not reliable in this angular region.

The experimental results may be combined in two ways in order to establish a comparison with a theoretical model. We plot P_n as a function of the mean charge $\bar{n}$, defined as $\bar{n} = \sum nP_n$; the result is that for both Ar and Cu this yields a universal set of curves, in which the positions of points are independent of primary energy (fig. 3). Comparison of fig. 3a and fig. 3b even indicates that the fraction of n times charged ions as a function of $\bar{n}$ does not differ markedly for Ar and Cu. A sensitive test consists in comparison of intersection points of different P_i curves in fig. 3a and fig. 3b. Experimental points are indicated in fig. 3. The reproducibility of the points is about 10% of their value for Cu and better than 10% for Ar.

A second type of information can be obtained by plotting $\bar{n}$ *vs* the mean total inelastic energy loss $\bar{Q}$.

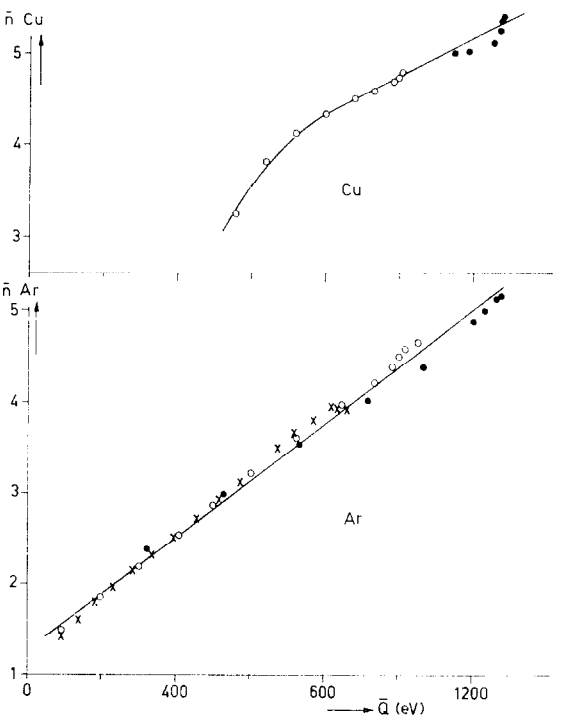

Fig. 4. The mean charge of Ar and Cu as a function of the mean total inelastic energy loss $\bar{Q}$.
Points are determined for different primary energies E_0.
×: $E_0 = 40$ keV, ○: $E_0 = 60$ keV, ●: $E_0 = 90$ keV.

We can determine $\bar{n}$ *vs* scattering angle from fig. 2; the dependence of $\bar{Q}$ on scattering angle is also known[5]), combination yields $\bar{n}$ as a function of $\bar{Q}$.

Curves of $\bar{n}_{Ar}$ and $\bar{n}_{Cu}$ *vs* $\bar{Q}$ are given in fig. 4.

Also in this case 3 different primary energies result in a universal curve for the two ion species under consideration.

4. *Phenomenological model for the Ar^+ on Cu collision.* We shall describe our measurements on the basis of the statistical model of Russek, extended by Everhart *et al.*[7]). The physical background of this model is:

1) The two approaching particles form a short living molecule, in which excitation of electrons takes place. Not in every collision at a certain primary energy and scattering angle the same inelastic energy is dissipated, but there is a distribution in inelastic energies.

2) The inelastic energy is distributed among the collision partners when they separate, both in an auto-ionizing state.

3) After separation de-excitation and electron emission takes place. In some cases a fast electron is emitted, according to the prediction by Fano and Lichten[9,10]). The remaining part of the inelastic energy is statistically distributed among the outer shell electrons, according to Russek's model.

We shall concern ourselves with a brief outline and a simple illustration of the statistical theory for the ionization probabilities.

The problem consists of randomly distributing an amount of energy E among N electrons and finding the probability that n electrons receive more energy than their respective ionization potentials.

4.1. Uniform ionization potential. In a simple approximation we take all ionization potentials equal. In fact the problem now reduces to a well known problem related to the random division of an interval. An interval of length E is divided into N subintervals by $N - 1$ points chosen at random on the line. The probability P_n^N that exactly n of the subintervals will exceed E_{ion} (which is the uniform ionization potential) is given by[11]):

$$P_n^N = \binom{N}{n} \sum_{i=n}^{N} (-1)^{i-n} \binom{N-n}{N-i} \left(1 - i\frac{E_{ion}}{E}\right)^{N-1}, \tag{1}$$

for $n = 0, 1, \ldots, N$, with the requirement:

$$\left(1 - \frac{iE_{ion}}{E}\right) \equiv 0 \qquad \text{for} \qquad \frac{iE_{ion}}{E} \geq 1.$$

This is Russek's formula (ref. 8, formula 6) for the nth ionization probability.

As an illustration for the derivation of (1) we treat the case that all N electrons over which the energy is distributed, are removed. We shall derive

the expression for P_n^N for the general case of nonequal ionization energies. The energy E is distributed among N electrons and let the energy received by the k-th electron be $\underline{E}_k$ then we have to find the probability that $\underline{E}_k \geq E_k$ for $k = 1, \ldots, N$, in which E_k are relevant ionization energies. In the final expression all E_k will be taken equal for the uniform ionization potential case. We assume a uniform probability density $P(\underline{E}_1, \underline{E}_2, \ldots, \underline{E}_{n-1})$, with the condition

$$\underline{E}_n = E - \sum_{k=1}^{N-1} \underline{E}_k \geq 0.$$

The volume in the $N - 1$ dimensional phase space is given by

$$\frac{1}{(N-1)!} E^{N-1}$$

and we have therefore

$$P(\underline{E}_1, \underline{E}_2, \ldots, \underline{E}_{N-1})\, \mathrm{d}\underline{E}_1, \mathrm{d}\underline{E}_2 \ldots \mathrm{d}\underline{E}_{N-1} = \frac{\mathrm{d}\underline{E}_1\, \mathrm{d}\underline{E}_2 \ldots \mathrm{d}\underline{E}_{N-1}}{\frac{1}{(N-1)!} E^{N-1}}. \tag{2}$$

Physically, this means that the matrix element for a transition from an initial (auto-ionizing) state to the final state in which an electron receives $\underline{E}$, does not depend on $\underline{E}$.

We can calculate the probability for N-fold ionization by

$$P_N^N = P(\underline{E}_1 > E_1, \underline{E}_2 > E_2, \ldots, \underline{E}_{N-1} > E_{N-1}; E - \sum_{k=1}^{N-1} \underline{E}_k > E_N) =$$

$$= \int_{E_1}^{E-E_2-E_3\ldots E_N} \int_{E_2}^{E-\underline{E}_1-E_3\ldots E_N} \cdots \int_{E_{N-1}}^{E-\underline{E}_1-\underline{E}_2\ldots\underline{E}_{N-2}-E_N} P(E_1, \underline{E}_2, \ldots, \underline{E}_{N-1}) \cdot$$

$$\cdot \mathrm{d}\underline{E}_1, \mathrm{d}\underline{E}_2 \ldots \mathrm{d}\underline{E}_{N-1} = \left(1 - \frac{\sum_{k=1}^{N} E_k}{E}\right)^{N-1}. \tag{3}$$

The integration intervals are determined by the requirement $\underline{E}_k > E_k$, while on the other hand the sum of all $\underline{E}_k$'s has to be E. We need $N - 1$ integrals because the choise of the first $N - 1$ energies determines the Nth. In case of a uniform ionization potential all E_k are equal to E_{ion}. Here P_N^N reduces to

$$P_N^N = \left(1 - \frac{NE_{\mathrm{ion}}}{E}\right)^{N-1}, \tag{4}$$

which satisfies relation (1).

An advantage of this method over Russek's derivation lays in the fact that the partition of energy E into units ε, with subsequent limit of ε to zero is avoided. The functions P_n^N plotted *vs* $\bar{n}$ can be found in Russek's paper (ref. 8, fig. 8). At a first glance they seem to describe the results $Ar^+ \rightarrow Ar$ and also our results (fig. 3) rather well. However, the dependence of P_n^N on excitation energy is incorrect, as may be expected from the rather crude assumption of a uniform ionization potential.

4.2. Staggered ionization potential. Also exact formulas for the ionization probabilities for the more realistic case of ionization potentials depending on the number of escaped electrons can be derived.

Russek assumes a simultaneous ionization of n electrons, which therefore (because of symmetry) all lose an energy equal to the mean of the first n ionization energies. This mean ionization energy appears to be a function of the inelastic (excitation) energy.

In contrast to this model we think that there exists a certain time order in which electrons receive energy. We label the electron which receives energy first as 1 *etc.* Let its energy be $\underline{E}_1$ and let the nth ionization energy be E_n as before. Now we are able to write down the ionization probabilities. The simplest case is, when no ionization occurs, only excited states result, which may de-excite by photon emission:

$$P_0^N = P(\underline{E}_1 < E_1, \underline{E}_2 < E_1, \ldots, \underline{E}_N < E_1). \tag{5}$$

The single ionization probability becomes

$$\begin{aligned} P_1^N = \{&P(\underline{E}_1 < E_1, \ldots, \underline{E}_{N-1} < E_1, \underline{E}_N \geq E_1) + \\ &+ P(\underline{E}_1 < E_1, \ldots, \underline{E}_{N-2} < E_1, \underline{E}_{N-1} \geq E_1, \underline{E}_N < E_2) + \ldots + \\ &+ P(\underline{E}_1 \geq E_1, \underline{E}_2 < E_2, \ldots, \underline{E}_N < E_2)\}. \end{aligned} \tag{6}$$

It consists of N terms, the first of which describes the possibility that the first $N - 1$ electrons receive an energy, not sufficient to overcome E_1 and the last electron escapes. The last term indicates ionization of the first electron, the remaining $N - 1$ electrons receiving an energy less than E_2.

Generally, the probability for n-fold ionization is a sum of $\binom{N}{n}$ terms. Mathematical expressions can be obtained for these terms.

The following relationship holds:

$$P(\underline{E} < E_k) = P(\underline{E} > 0) - P(\underline{E} > E_k). \tag{7}$$

By repeated application of (7) all terms in the expressions for the ionization probabilities can be written as linear combination of terms $P(\underline{E}_1 \geq e_1, \underline{E}_2 \geq e_2, \ldots, \underline{E}_n \geq e_n)$, in which the e_i may be ionization energies or zero, these terms containing no "$<$" relations.

For these terms we already derived expression (3). The result is that all

ionization probabilities in the staggered ionization energy case can be written as a linear combination of terms of the form (3).

For the ionization energies we use the simple approximation $E_k = kE_1$, which means that after removal of $k-1$ electrons the effective charge which the next electron experiences is k times the charge acting upon the most weakly bound electron. In this case a closed expression can be given for the ionization probabilities:

$$P_n^N = \sum_{j=0}^{N-n} (-1)^j \binom{N}{n+j} \sum_{m=\frac{1}{2}n(n+1)}^{\frac{1}{2}n(n+1)+nj} c\,(n, j; m - \tfrac{1}{2}n(n+1)) \times \\ \times (1 - (m+j)\,E_1/E)^{N-1}. \tag{8}$$

This distribution satisfies the normalization condition

$$\sum_{n=0}^{N} P_n = 1.$$

The coefficients $c(i, j; k)$ originate from the repeated application of (7) and they can easily be found by recursion:

$$c(i, j; k) = c(i-1, j; k) + c(i, j-1; k-i), \tag{9}$$

with initial conditions:

$$c(i, j; k) = 0 \qquad \text{if} \qquad i, j, \text{ or } k \text{ is negative}$$

$$c(i, 0; k) = c(0, j; k) = \delta_{0k} \qquad \text{for non-negative } i, j \text{ and } k.$$

Because we use ions as a projectile, we also have to calculate ionization probabilities of an *ion*, P_n^N (ion). Now the lowest energy which electrons need for ionization is the *second* ionization potential.

The result is:

$$P_n^N \text{ (ion)} = \sum_{j=0}^{N-n} (-1)^j \binom{N}{n+j} \times \\ \times \sum_{m=\frac{1}{2}n(n+1)}^{\frac{1}{2}n(n+1)+nj} c(n, j; m - \tfrac{1}{2}n(n+1))(1 - (m+n+2j)\,E_1/E)^{N-1}. \tag{10}$$

After the formation of the quasi molecular complex, it is not known which of the particles is missing the electron.

Let the electron-capture probability during the collision be a, then the resulting expression for the fraction of n times charged ions is:

$$P_n = aP_n^N + (1-a)\,P_{n-1}^{N-1} \text{ (ion)}. \tag{11}$$

P_n is a function of n, N, the first ionization potential E_1, the capture probability a and the amount of excitation energy E which the atom (or ion) receives during the collision.

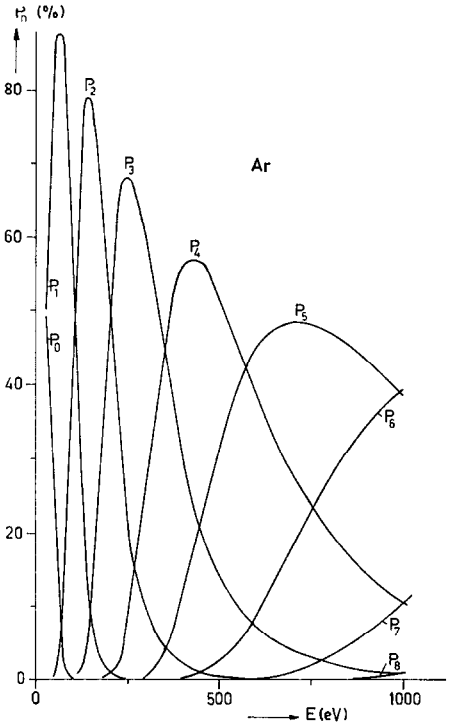

Fig. 5. P_n functions for Ar, calculated from formula (11), plotted as a function of excitation energy E, dissipated in Ar.

Surprisingly, calculation of expressions (8) and (9) and combination by (11) for different capture probabilities showed that P_n is nearly independent of a.

In the case of a symmetric collision (for instance $Ar^+ \rightarrow Ar$) it is reasonable to take $a = \frac{1}{2}$, but in our case ($Ar^+ \rightarrow Cu$) a is unknown. Therefore the independence of P_n on a is a favourable circumstance.

As an illustration of a calculation of P_n functions by formula (11) we show in fig. 5 ionization probabilities of Ar as a function of excitation energy E. For this case $N = 8$, $E_1 = 16$ eV and $a = \frac{1}{2}$.

5. *Distribution in inelastic energy.* It is known from measurements by Kessel *et al.*[1]) and Snoek *et al.*[5]) that the total inelastic energy Q dissipated during the collision in both scattering partners for fixed impact parameter and primary energy shows a broad distribution.

Everhart *et al.*[7]) assume this distribution to be Gaussian and measured the width as a function of $\bar{Q}$, the mean of the distribution.

The inelastic energy is shared by the collision partners, the distribution in Q resulting in distributions in the excitation energies which both partners receive. In case of identical collision partners the width of the distribution

in excitation energy in one particle can be related to the width of the distribution in *total* Q. Again, in our unsymmetrical case it is not known in which way Q is distributed over both particles. Filippenko[12]) indicates that the ratio of energies given to the two particles is the ratio of the number of outer-shell electrons in the collision partners. In the case of Cu which has one (4s) electron in its outer-shell this rule seems hardly applicable.

Therefore we made the assumption that both partners receive half of the mean total inelastic energy $\bar{Q}$. The normalized distribution in excitation energy E around the mean $\bar{E} = \frac{1}{2}\bar{Q}$ is given by

$$f(E)\,\mathrm{d}E = \frac{1}{\sigma(E)\sqrt{2\pi}}\,\mathrm{e}^{-(E-\bar{E})^2/\sigma^2(E)}\,\mathrm{d}E. \tag{12}$$

If $\bar{E} = \frac{1}{2}\bar{Q}$ and if both distributions are Gaussian, the width $\sigma(\bar{E})$ is related to the width in the distribution of Q like[7]) $\sigma(\bar{E}) = 2^{-\frac{1}{2}}\sigma(\bar{Q})$.

Measurements of $\sigma(\bar{Q})$ *vs* $\bar{Q}$ for the case of $Ar^+ \rightarrow Cu$ are presented in ref. 5, the result is that $\sigma(\bar{E})$ is approximately linearly dependent on $\bar{E}$:

$$\sigma(\bar{E}) = 0.43\bar{E}. \tag{13}$$

It is interesting to note that the case $Ar^+ \rightarrow Ar$ leads to roughly the same relation between $\sigma(\bar{E})$ and $\bar{E}$, see ref. 7, fig. 3a.

Mark that the assumption $\bar{E} = \frac{1}{2}\bar{Q}$ is only made to obtain $\sigma(\bar{E})$ and is of minor importance for the calculation of P_n curves.

6. *Comparison of calculated and measured P_n functions.* We calculate the ionization probabilities, resulting from statistical distribution of inelastic energy, which itself is normally distributed, in the following way:

$$\overline{P_n(E)} = \int P_n(E)\, f(E)\, \mathrm{d}E, \tag{14}$$

in which $P_n(E)$ and $f(E)$ are given by expressions (11) and (12), respectively.

For the case of Ar we evaluate (11) with $N = 8$ and $a = \frac{1}{2}$, the k-th ionization potential we take as k times the first, E_1, which is 16 eV. In Russek's paper it is shown that this is a rather good approximation.

Now we plot $\bar{P}_n$ *vs* $\bar{n}$, these curves are compared with the measured ones in fig. 6a.

For Cu we took $N = 11$, thus assuming the ten 3d electrons and a 4s electron to partake in the distribution of energy, because the closed 3d shell shields the deeper laying 3p and 3s shells.

The choice of N, however, is not so important for the following reason. It is observed that the distribution P_n^N (formula (8)) becomes nearly independent on N for $N > 7$. In fact the P_n^N are closely approximated by a normal distribution around $\bar{n}$, the width *not* depending on N.

The ionization potentials are taken as k times 10 eV, which overestimates the first ionization potential (7.8 eV), it correctly describes the second and

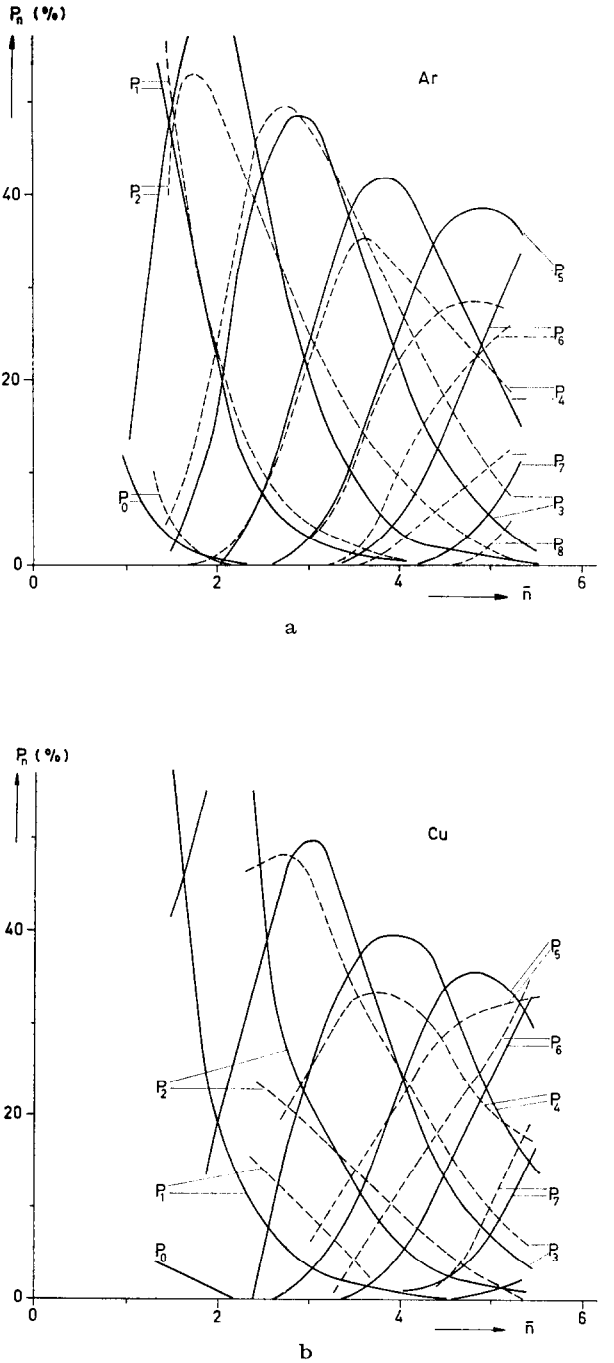

Fig. 6. Comparison of theoretical (formula (14)) and experimental P_n functions for Ar (a) and Cu (b).
Calculated curves are full lines.

underestimates the next potentials ($E_2 = 20$ eV, $E_3 = 36$ eV, higher potentials are not known).

Figure 6b compares calculated and measured P_n functions for Cu.

For the higher-charge states, the calculated values lie generally above the measurements. Apart from the imperfections in the model, this may be due to charge changing of highly charged scattering products in the vicinity of walls and slits. This charge changing is the most probable for the higher-charge states (see following paper[13])).

7. *Fast electrons.* It is known that violent atomic collisions produce excitation of inner shell electrons[9]). Direct evidence is provided by the occurrence of fast electrons. The probability for Ar L-shell excitations has been measured for the $Ar^+ \rightarrow Ar$ case as a function of r_0, the distance of closest approach in the collision[1]). Here electrons with energy near 200 eV occur. In the case of $Ar^+ \rightarrow Cu_{solid}$ 200 eV electrons resulting from Ar L-shell excitations also have been measured[10]). Radiation from Ar L-de-excitation has been found recently for the case of $Ar^+ \rightarrow Cu_{solid}$ (ref. 14).

On the other hand, a steep rise in the curve of mean inelastic energy loss $\bar{Q}$ *vs* r_0 has not been found for $Ar^+ \rightarrow Cu$ collisions. Probably because of the dissimilarity of the electron clouds of the colliding atoms in the $Ar^+ \rightarrow Cu$ case the structure is spread out over an extended region of r_0. Consequently we cannot estimate the probability for the creation of an L-shell vacancy.

In the P_n curves, presented in this paper, one does not observe discontinuities also indicating a spreading of the effect. Experimental evidence, therefore, is insufficient to incorporate the occurrence of fast electrons in the calculation of the P_n curves.

8. *Consistency check of the model and conclusion.* Plotting of P_n curves *vs* mean charge obscures the dependence on the excitation energy. We have, however, an indirect way to compare the dependence of P_n on excitation energy (as calculated) with the dependence of the measured P_n on the *total* inelastic energy $\bar{Q}$.

The experimental dependence of $\bar{Q}$ on $\bar{n}$ is known for Ar and Cu (fig. 4). We are also able to calculate separately for both Ar and Cu how much energy is needed to create a mean charge $\bar{n}_{Ar}$ in Ar and $\bar{n}_{Cu}$ in Cu. The sum of these calculated energies must add up to $\bar{Q}$.

In fig. 7 is indicated the part of $\bar{Q}$ which is received by Ar and the fraction used by Cu. The sum yields 90 to 105% of $\bar{Q}$ for a large region of Q. In the uniform ionization potential $E_{Ar}/\bar{Q}$ alone already exceeds 100% for a uniform ionization potential of 30 eV. So in conclusion it may be stated that the used model sufficiently well describes the results.

On one hand the charge state probabilities are reasonably well described

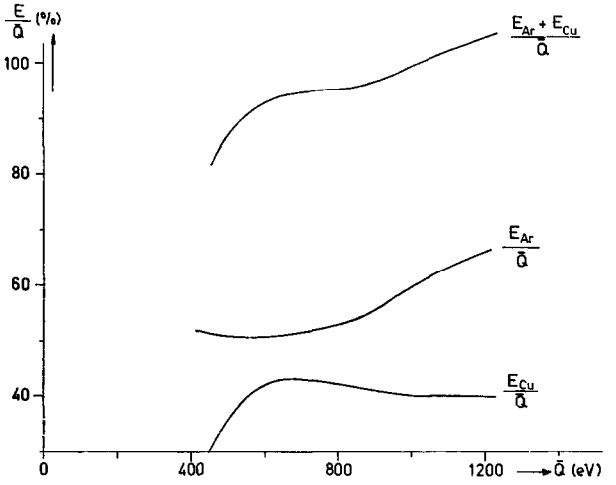

Fig. 7. Fractions of mean total inelastic energy, dissipated in Ar and Cu, respectively, $E_{Ar}/\bar{Q}$ and $E_{Cu}/\bar{Q}$. The sum $(E_{Ar} + E_{Cu})/\bar{Q}$ is also indicated.

and on the other hand it is shown that nearly 100% of the total inelastic energy loss is consumed into both partners for excitation and ionization.

Acknowledgments. We wish to thank Prof. J. Kistemaker, Prof. A. Russek, Dr. C. Snoek and Drs. F. W. Saris for many stimulating discussions.

The help of S. Doorn and H. H. Roukens in carrying out the experiments is gratefully acknowledged.

Computer calculations were performed with the X8 computer of the Mathematisch Centrum, Amsterdam.

This work is part of the research program of the Stichting voor Fundamenteel Onderzoek der Materie (Foundation for Fundamental Research on Matter) and was made possible by financial support from the Nederlandse Organisatie voor Zuiver Wetenschappelijk Onderzoek (Netherlands Organization for the advancement of Pure Research).

REFERENCES

1) Kessel, Q. C. and Everhart, E., Phys. Rev. **146** (1966) 16.
2) Afrosimov, V. V., Gordeev, Iu. S., Panov, M. N. and Fedorenko, N. V., Zh. tekh. Fiz. **34** (1964) 1613, 1624, 1637; English transl.: Soviet Physics – Technical Physics **9** (1965) 1248, 1256, 1265.
3) Datz, S. and Snoek, C., Phys. Rev. **134** (1964) A 347.
4) Dahl, P. and Magyar, J., Phys. Rev. **140** (1965) A 1420.
5) Snoek, C., Van der Weg, W. F., Geballe, R. and Rol, P. K., Physica **35** (1967) 1.
6) Snoek, C., Van der Weg, W. F., Geballe, R. and Rol, P. K., Proc. 7th Int. Conf. on Phenomena in Ionized Gases, Belgrade, 1966, p. 145.

7) Everhart, E., and Kessel, Q. C., Phys. Rev. **146** (1966) 27.
8) Russek, A., Phys. Rev. **132** (1963) 246.
9) Fano, U. and Lichten, W., Phys. Rev. Letters **14** (1965) 627.
10) Snoek, C., Geballe, R., Van der Weg, W. F., Rol, P. K. and Bierman, D. J., Physica **31** (1965) 1553.
11) E. Parzen, Modern Probability Theory and its Applications, Wiley (New York, 1964) p. 306.
12) Filippenko, L. G., Zh. tekh. Fiz. **32** (1962) 356. English transl.: Soviet Physics – Technical Physics **7** (1962) 254.
13) Van der Weg, W. F. and Bierman, D. J., Physica **44** (1969) 177.
14) Saris, F. W., Van der Weg, W. F. and Onderdelinden, D., to be published in Radiation Effects.